Quasiclassical Trajectory Simulations of OH(v) + NO2 → $HONO_2$* → OH(v′) + NO_2: Capture and Vibrational Deactivation Rate Constants

Yong Liu,[†,‡] Lawrence L. Lohr,[§] and John R. Barker*[,†,§]

Department of Atmospheric, Oceanic, and Space Sciences, University of Michigan, Ann Arbor, Michigan 48109-2143, and Department of Chemistry, University of Michigan, Ann Arbor, Michigan 48109-1055

Received: June 9, 2005; In Final Form: November 14, 2005

Quasiclassical trajectory calculations are used to investigate the dynamics of the OH(υ) + NO_2 → $HONO_2$* → OH(υ') + NO_2 recombination/dissociation reaction on an analytic potential energy surface (PES) that gives good agreement with the known structure and vibrational frequencies of nitric acid. The calculated recombination rate constants depend only weakly on temperature and on the initial vibrational energy level of OH(υ). The magnitude of the recombination rate constant is sensitive to the potential function describing the newly formed bond and to the switching functions in the PES that attenuate inter-mode interactions at long range. The lifetime of the nascent excited $HONO_2$* depends strongly not only on its internal energy but also on the identity of the initial state, in disagreement with statistical theory. This disagreement is probably due to the effects of slow intramolecular vibrational energy redistribution (IVR) from the initially excited OH stretching mode. The vibrational energy distribution of product OH(υ') radicals is different from statistical distributions, a result consistent with the effects of slow IVR. Nonetheless, the trajectory results predict that vibrational deactivation of OH(υ) via the $HONO_2$* transient complex is ∼90% efficient, almost independent of initial OH(υ) vibrational level, in qualitative agreement with recent experiments. Tests are also carried out using the $HONO_2$ PES, but assuming the weaker O−O bond strength found in HOONO (peroxynitrous acid). In this case, the predicted vibrational deactivation efficiencies are significantly lower and depend strongly on the initial vibrational state of OH(υ), in disagreement with experiments. This disagreement suggests that the actual HOONO PES may contain more inter-mode coupling than found in the present model PES, which is based on $HONO_2$. For nitric acid, the measured vibrational deactivation rate constant is a useful proxy for the recombination rate, but IVR randomization of energy is not complete, suggesting that the efficacy of the proxy method must be evaluated on a case-by-case basis.

1. Introduction

Consider what happens in a typical radical + radical recombination reaction. As the two radicals approach one another on the potential energy surface (PES), a new chemical bond begins to form, releasing chemical energy into the reaction coordinate (identified with the newly forming bond). In order for the new molecule to survive, some of the energy must be redistributed within a single vibrational period to other internal degrees of freedom. Otherwise, the newly formed molecule will simply redissociate. If the molecule survives for the first vibrational period, further intramolecular vibrational energy redistribution (IVR) can take place, perhaps eventually resulting in complete randomization of energy. At any time during this process, redissociation may occur if enough energy concentrates in the reaction coordinate. If collisions are frequent enough, they may intervene and remove energy, stabilizing the new molecule. At the high-pressure limit of a recombination reaction, *every* newly formed molecule is stabilized by collisions before redissociation can occur.

In the absence of energy transfer collisions, energy initially in a vibrationally excited reactant will tend to be randomized by IVR prior to redissociation of the new molecule. If IVR is fast enough in a molecule that contains at least four to five atoms, the randomized energy will be spread over many degrees of freedom and there will be little statistical chance that vibrational energy will be concentrated in any particular product vibrational mode, effectively resulting in vibrational deactivation of the initial vibrationally excited reactant. Thus, there is an intimate connection between capture (formation of the newly formed molecule), IVR, the high-pressure limit of a recombination reaction rate constant k_∞, and vibrational deactivation.

In light of this picture of a recombination reaction, Quack and Troe[1] and Smith and co-workers[2,3] have suggested that the rate constant for vibrational deactivation of excited free radicals can be identified with k_∞ when the vibrational deactivation takes place via formation of a "strongly coupled complex" (defined as the newly formed molecule with energy completely randomized by IVR). This suggestion that vibrational deactivation may be used as a proxy for the high-pressure limit has important practical implications because of the great difficulties associated with measuring k_∞.

In the present work, we examine the dynamics of capture, IVR, and redissociation in order to determine the quantitative relationship between k_∞ and k_υ, the rate constant for vibrational

* Address correspondence to this author. E-mail: jrbarker@umich.edu.
† Department of Atmospheric, Oceanic, and Space Sciences, University of Michigan.
‡ Present address: Pacific Northwest National Laboratory, P.O. Box 999, Richland, WA 99352.
§ Department of Chemistry, University of Michigan.

10.1021/jp053099a CCC: $33.50
Published on Web 12/14/2005

deactivation. Our ultimate aim is to ascertain under what conditions the proxy method will be of value.

The proxy method will only be useful when vibrational deactivation via formation of a strongly coupled complex is much more efficient than other possible collisional energy transfer mechanisms.[3] Energy transfer, such as that which dominates in collisions between excited hydrogen halides and monatomic gases, is well-known.[4−7] It is characterized by rather small rate constants, because the collisions are not sufficiently impulsive (collision duration much shorter than the vibrational period) during a thermal collision when the repulsive intermolecular potential energy is of typical steepness as a function of intermolecular distance.[6] Furthermore, the rate constant scales approximately with the vibrational quantum number of the upper state. The OH(v) radical is similar to hydrogen halides in this regard, having small rate constants at low v for vibrational deactivation (which scale approximately with v) in collisions with nonreactive gases.[8] Vibration-to-vibration energy transfer may also take place, but it is rapid only when the two collision partners have nearly resonant vibration frequencies,[5,6] which is not the case for OH and NO_2.

Our work is motivated in part by the recent interest in the OH + NO_2 recombination reaction, which plays a central role in controlling free radical concentrations in the troposphere and stratosphere. Nitric acid, one product of the reaction between OH and NO_2, is a principal sink for atmospheric NO_x (the sum of NO and NO_2) and OH. Since photolysis of NO_2 produces odd oxygen (O_x, the sum of O and O_3), reaction 1a has a direct impact on both tropospheric and stratospheric ozone concentrations. Because of this key role, the OH + NO_2 reaction has received much attention and a large body of experimental data exists.[9−13] Although many data have been obtained at relatively high pressure, extrapolation of the falloff curves toward the high-pressure limiting rate constant k_∞ is still uncertain. Moreover, recent experiments[14,15] have unambiguously confirmed a second reaction channel that was previously surmised[16,17] to produce peroxynitrous acid (HOONO). Reaction 1b is probably of only indirect importance in the atmosphere because of the short lifetime and likely fate of HOONO.[18] However, most of the reported rate constants were measured by observing the rate of loss of OH radicals, which corresponds to the sum of rates via the two channels. The direct isomerization between HOONO and $HONO_2$ in the gas phase is thought to be negligible[19−21] because of the high energy barriers found in theoretical studies[22−24] and the very low measured yield of $HONO_2$ produced in the reaction of HO_2 with NO.[25] Thus, the contribution from reaction 1b must be known in order to determine the rate constant for reaction 1a.

$$\mathrm{OH} + \mathrm{NO_2}\ (+\mathrm{M}) \rightleftharpoons \mathrm{HONO_2}\ (+\mathrm{M}) \qquad (1a)$$

$$\mathrm{OH} + \mathrm{NO_2}\ (+\mathrm{M}) \rightleftharpoons \mathrm{HOONO}\ (+\mathrm{M}) \qquad (1b)$$

In recent theoretical analyses[21,26] and master equation calculations,[20] statistical theory was used to extrapolate pressure-dependent rate constants measured for reaction 1 to the high-pressure limit (k_∞). Troe predicted that the temperature dependence of $k_{1\infty}$ over the temperature range 50−1000 K is only a few percent, due to compensations of small temperature dependences of centrifugal partition function, electronic partition function and the so-called thermal rigidity factor.[21] The available experimental data are not sufficient to determine the temperature dependence of $k_{1\infty}$. One goal of the present study is to investigate this temperature dependence.

The central goal of this work is to evaluate the proxy method for determining k_∞ suggested by Quack and Troe[1] and by Smith and co-workers,[2] as described above. According to this suggestion, the vibrational deactivation rate constant k_v measured for reaction 2 may be used as a proxy for the high-pressure limiting rate constant for reaction 1

$$\mathrm{OH}(v) + \mathrm{NO_2} \rightarrow \mathrm{OH}(v') + \mathrm{NO_2} \qquad (2)$$

where v and v' are vibrational quantum numbers for the OH radical. Here, the vibrational deactivation is mediated by the vibrationally excited transient $HONO_2$* complex (asterisk denotes internal excitation) in which the energy is randomized and there is only a small statistical probability that $v' = v$. In recent measurements of vibration relaxation of OH(v) by NO_2 at low pressures, Hynes and co-workers[27−29] have found that the rate constant k_v is almost independent of v. This finding is consistent with the randomization of energy in a strongly coupled complex and differs from the v-scaling expected for energy transfer by nonreactive gases. A goal of the present work is to investigate the quantitative relationship between k_∞ and k_v for reactions 1a and 2, respectively, for a range of model PESs for HO−NO_2.

In the present work, we use quasiclassical trajectory calculations to investigate the process of capture, redistribution of energy, and consequent vibrational deactivation of initially excited radicals. This dynamical method makes no statistical assumptions, is useful for simulating IVR, and is capable of determining whether vibrational deactivation is the result of capture, or other mechanisms. Despite their known limitations,[30−32] classical trajectories have been widely used in modeling reaction dynamics, collisional energy transfer, and intramolecular vibrational energy redistribution (IVR).[33−40] In particular, quasiclassical trajectory methods have been used successfully in studying ion−molecule and radical−radical recombination reactions.[41−43] Classical trajectory methods cannot accurately simulate quantum zero point energies and interference phenomena. These effects are of reduced importance at the high internal energies of the excited nascent $HONO_2$ molecule (∼53−70 kcal mol^{-1}), compared to its zero point energy (∼16.5 kcal mol^{-1}). Although quantum statistics differ from the classical analogue,[32] the two are not greatly different at these high energies. In the quasiclassical method, the initial conditions of the classical trajectories are selected to correspond to quantum states of the reactants. Final "quantum" state distributions are obtained by "binning" the classical product energies with energy bins centered on the quantum state energies.[44] This procedure is not sophisticated,[45] but it produces reasonable results when the final energy distributions are relatively broad.

The present calculations employ slightly modified versions of an analytical potential energy surface (PES) for $HONO_2$, which is based on the measured equilibrium structure, measured vibrational frequencies, and ab initio quantum chemical calculations.[40] This PES is in very good agreement with the measured equilibrium properties of nitric acid. Attenuation terms were determined from ab initio calculations using the Gaussian-98 program[46] at the level of quadratic configuration interaction with single, double, and perturbative corrections for triple excitations[47] with the correlation consistent polarized valence triple-ζ basis set of Dunning[48] (QCISD(T)/cc-pvtz). Using this PES, the calculated intramolecular vibrational energy redistribution (IVR) time constant[40] following initial excitation of O−H overtone vibration ($v_{OH} = 2$) in $HONO_2$ is in excellent agreement with the experimental value.[49] Although this PES neglects the existence of HOONO, it should still provide insights into the dynamics of reaction 1a.

TABLE 1: Potential Energy Parameters That Differ from Those in Table 1 of Reference 40[a]

PES	value
standard	$D_3 = 51.30$ kcal/mol; $\beta_3 = 2.155$ Å^{-1}
stiff	$D_3 = 51.30$ kcal/mol; $C_{31} = 2.17$ Å^{-1}; $C_{32} = 0.12$ Å^{-2}; $C_{33} = 0.50$ Å^{-3}; $C_{34} = 0.0$
stiffer	$D_3 = 51.30$ kcal/mol; $C_{31} = 2.17$ Å^{-1}; $C_{32} = 0.18$ Å^{-2}; $C_{33} = 1.40$ Å^{-3}; $C_{34} = 0.0$

[a]See ref 40 for definitions of notation.

In this work, we consider two criteria for "capture" during a classical trajectory and show that the calculated capture rate constants k_{cap} are not very sensitive to the choices of how the criteria are applied. The capture rate constant can be identified with k_∞ because at the high-pressure limit every complex formed by capture will be deactivated by collisions. Trajectory calculations are used to obtain capture rate constants from 200 to 1500 K for initial OH(v) vibrational states from $v = 0$ to $v = 5$. Lifetimes of the transient vibrationally excited $HONO_2$* complexes are calculated and used to estimate the corresponding dissociation rate constants. The vibrational states of OH(v') produced by redissociation of the transient complex are determined by binning the trajectory results. Both the redissociation rate constants and the OH(v') vibrational energy distributions clearly show the influence of incomplete IVR. Nevertheless, the calculations support the practical utility of the proxy method,[1,2] in agreement with the experimental measurements of Hynes and co-workers.[27−29]

2. Quasiclassical Trajectory Method

2.1. Potential Energy Surface. The present work relies on a modified version of the well-established VENUS96 trajectory code[50] in which the potential energy is formulated in terms of curvilinear internal coordinates and then transformed to a Cartesian coordinate frame. With this procedure the accuracy of the Hamiltonian depends only on the potential energy, since no terms are neglected in the kinetic energy expression.[33]

The Born−Oppenheimer PES for nitric acid used in this work was constructed with a many-body expansion approach.[51] The notation, parameters, and other details of the $HONO_2$ analytic PES have been reported elsewhere.[40] The present PES is almost the same as the one used previously, except two of the parameters[40] in the O−N Morse potential function for the newly formed HO−NO_2 bond were revised slightly to give the present values: $D_3 = 51.03$ kcal/mol and $\beta_3 = 2.155$ Å^{-1} (see Table 1). The differences result from the use of D_e instead of D_0 in the O−N Morse potential function. With these small revisions in the PES, the calculated IVR time constants are within 5% of the values reported previously.[40] In the present work, this revised PES is considered our "standard" PES for the reaction.

The principal goal here is to study the recombination reaction; therefore, accurate asymptotic behavior of the PES at long distance is important. For that reason, the analytic PES is based on the dipole moments of NO_2 and OH radical so that the electrostatic interactions are reasonably accurate at long range.[40] The potential energy function at intermediate ranges is particularly important. But ab initio calculations at the single determinant level of theory used here (see below) do not yield accurate results for the O−N bond lengths greater than 2.0−3.0 Å. Higher levels of theory are very expensive and of uncertain accuracy. Therefore, we constructed a family of model PESs with various long-range behaviors and carried out sensitivity tests to determine the effect of the long-range behavior on the calculated rate constants. In the development of the model PESs, we used a generalized Morse function, one

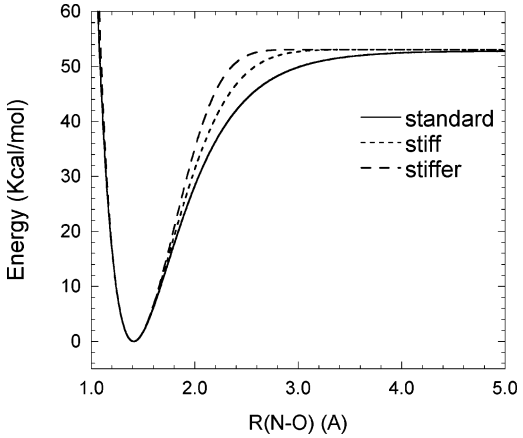

Figure 1. Plot of "standard", "stiff", and "stiffer" Morse potentials.

TABLE 2: Impact Parameters and Capture Numbers (out of 10^4 Trajectories) for the Recombination Reaction as a Function of Temperature

temp (K)	b_{max} (Å)	N_r
200	4.3	888
300	4.0	1199
500	4.0	1488
800	4.0	1636
1000	3.6	2075
1200	3.4	2292
1500	3.4	2159

of the built-in functions in VENUS, to model the O−N stretching mode. In the standard Morse potential, parameter β is a constant (see above). In VENUS, the generalized Morse potential parameter β is represented by a cubic polynomial function of the O−N displacement from equilibrium:

$$V_{GM}(r) = D_e(1 - e^{-\beta}\Delta r)^2 \quad (3a)$$

$$\beta = c_1 + c_2\Delta r + c_3\Delta r^2 + c_4\Delta r^3, \Delta r = r - r_0 \quad (3b)$$

where D_e is the bond dissociation energy and r_0 is the equilibrium bond distance. Appropriate choices of parameters in eq 3b can produce a potential that rises toward the dissociation energy at a faster rate than the standard Morse function: the "stiff" Morse potential.[41] Trajectory calculations show that the calculated rate constants are sensitive to these parameters[41] (also see below). By varying the polynomial function, we can adjust the long-range behavior of the O−N bond without significantly varying the harmonic frequency. In this way, we generated PESs designated "standard", "stiff", and "stiffer" (see Table 1 and Figure 1). Harmonic normal-mode frequencies for $HONO_2$ calculated from this set of PESs are in excellent agreement with ab initio calculations and experimental results (Table 2 of ref 40). The equilibrium geometry of $HONO_2$ agrees well with the ab initio results and our previous work.[40] The maximum errors in bond distances and angles are <0.02 Å and $< 1.2°$, respectively.

As discussed below, the calculated rate constants are sensitive to choices of parameters associated with angular motions. In particular, "switching functions" are used to attenuate or otherwise modify force constants of bending and torsional modes as the molecule undergoes bond fission. For example, the bending mode force constant in a triatomic molecule ABC should vanish when the B−C bond is broken and the AB and C fragments are moved to infinite distance. Sensitivities of the calculated rate constants were investigated for variations in the switching function parameters for ∠HON bending (θ_1), ∠ONO

bending (θ_2 & θ_3), HONO torsion and ONOO wag modes. The atom-numbering scheme and the original parameters for the analytic PES are listed in Table 1 of ref 40.

2.2. Method for Determination of k_∞. Quasiclassical trajectory calculations are used to obtain capture rate constants by employing the standard expression[52]

$$k'_{cap}(T) = \left(\frac{8kT}{\pi\mu}\right)^{1/2} \pi b_{max}{}^2 \left(\frac{N_r}{N}\right) \quad (4)$$

where μ is the reduced mass of the reactants (OH and NO_2), N_r is the number of trajectories that form a capture complex, N is the total number of trajectories in the ensemble, and b_{max} is the maximum impact parameter. This equation neglects the influence of electronic degeneracy. When electronic degeneracy is included, the rate constant is

$$k_{cap} = k'_{cap}/g_e(T) \quad (5)$$

where $g_e(T)$ is the electronic degeneracy factor, which is equal to the product of the reactant electronic partition functions divided by the electronic partition function of the product. The ground electronic states of the reactants are $OH(X^2\Pi)$ and $NO_2(\tilde{A}^2B_2)$, but excited states can also contribute in a thermal system. Here it is assumed that the $HONO_2(X^1A')$ potential energy surface correlates with only one of the numerous potential energy surfaces originating from OH + NO_2. Since the electronic partition function of $HONO_2(X^1A')$ is equal to unity, the factor $g_e(T)$ is the product of the reactant electronic partition functions, where the first and second factors are the partition functions for OH and for NO_2, respectively:[53]

$$g_e(T) = [2 + 2\exp(-201/T)][2 + 2\exp(-13997/T)] \quad (6)$$

The collision impact parameter b is chosen by VENUS according to

$$b = b_{max} R^{1/2} \quad (7)$$

where R is a random number distributed uniformly between 0 and 1. The maximum impact parameter b_{max} is determined empirically in order to include ≥95% of complex-forming trajectories (for a thermal relative velocity distribution).

For present purposes, a captured trajectory is defined as one in which the HO−NO_2 distance is less than r_{crit} = 2.5 Å and the relative motion of the two reactants exhibits three or more inner turning points. This definition is arbitrary, but trial trajectory calculations showed that the capture number only changes by ~10% when r_{crit} is reduced to 2.2 Å or increased to 2.8 Å. Furthermore, the capture number is decreased by less than 10% if the selection criterion is increased to five inner turning points. This lack of sensitivity to the capture criteria is consistent with the lifetime distributions (see below), which indicate that most vibrationally excited $HONO_2$* complexes are relatively long-lived.

In this work, batches of N = 10 000 trajectories are used to determine the capture number N_r. Trajectories are averaged over phases and integrated for 2×10^6 time steps with a step size of 0.1 fs. The initial rotational and relative translational energies of the reactants are chosen from thermal distributions. Initial conditions for the vibrations were selected using microcanonical normal mode sampling. All of the sampling of initial conditions was carried out by VENUS.[50]

3. Results

3.1. Capture Rate Constants. The maximum impact parameters b_{max} and capture number N_r for each temperature are listed in Table 2. As shown, b_{max} decreases with increasing temperature because the centrifugal maximum of this barrierless reaction moves inward as the temperature (and relative speed) is increased. In contrast, the capture number increases with temperature (see discussion below). At all temperatures, ~10−20% of the trajectories result in formation of a $HONO_2$ complex. The capture rate constants obtained from eq 4 are shown in Figure 2. For the temperature range from 200 to 1500 K, the capture rate constants exhibit a weak increase with increasing temperature: the capture rate constant at 1500 K is about three times that calculated at 200 K. The temperature dependences can be reasonably fitted by the Arrhenius equation. Figure 2 also presents capture rate constants calculated for OH(υ) in initial vibrational states from υ = 0 to υ = 5. It is found that the capture rate constants are essentially independent of υ, indicating the formation of a complex is dominated by the long-range potential and not by the internal dynamics of the complex.

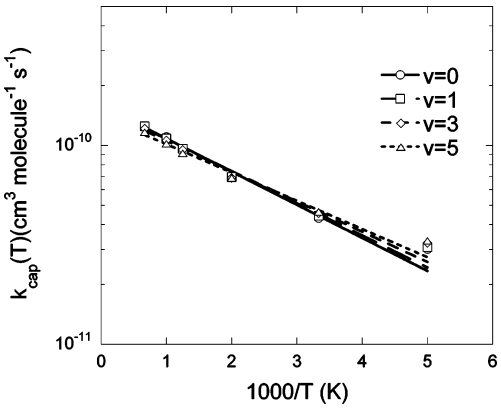

Figure 2. Capture rate constants calculated with different initial OH excitation energy over temperature range of 200−1500 K (standard PES).

At 300 K, the capture rate constant (corrected for electronic degeneracy) of the reaction of OH(υ = 0) with NO_2 is (7.1 ± 2.7) × 10^{-12} cm^3 mol^{-1} s^{-1} for the standard PES, about one-fourth of the value estimated for $k_{1\infty}$ on the basis of master equation simulations of laboratory data.[20] At high pressure, HOONO formation is believed to contribute in the experiments, but unfortunately the high-pressure rate constant for HOONO formation is not well determined.[20] Thus, some of the difference between the rate constants calculated here and ones based on experiments may be due in part to uncertainty in the rate of HOONO formation. However, most of the difference is probably due to inadequacies in the standard PES for the reaction. As will be discussed in the next section, plausible adjustments of some parameters can produce better agreement, but we again emphasize that our goal is not to produce agreement with measured rate constants, but to investigate the temperature dependence and the relationship between k_∞ and k_υ.

3.2. Sensitivity Tests of the PES. Since we do not have confidence that the single determinant quantum chemical methods provide accurate PESs at long range,[40] where the capture rate constant is determined, our approach is to obtain a set of PESs that span a range of plausible behaviors. Calculated capture rate constants for each of the three PESs (standard, stiff, and stiffer) are shown in Figure 3. It is clear that the behavior of the HO−NO_2 bond potential at intermediate to long range has a major influence on the calculated recombination rate constants. Rate constants based on the stiff and stiffer PESs are less than 10% as large as those based on the standard PES. This is probably because the stiff and stiffer PESs do not extend

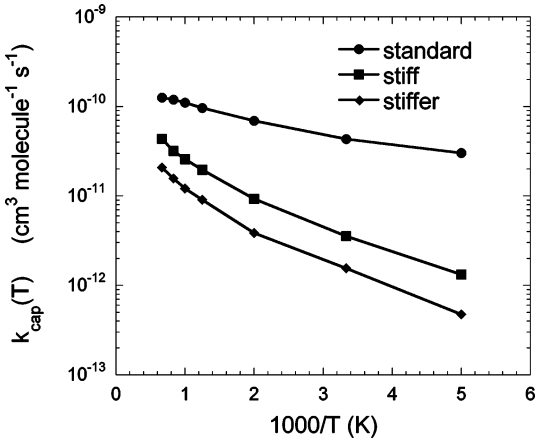

Figure 3. Capture rate constants as a function of temperature from different PESs.

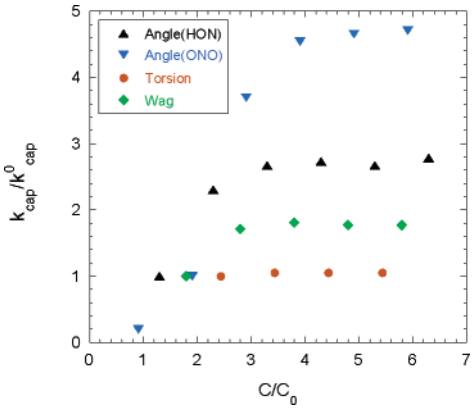

Figure 4. Effects of parameters in switching functions on capture rate constants (k°_{cap} = standard k_{cap}).

to such large distances (see Figure 1). These results are consistent with results found previously for the H + CH_3 reaction by Duchovic et al.[41]

Switching functions in the PES are also extremely important for ensuring that bending force constants and internal rotation barriers vanish appropriately when the reactants or products are separated by great distances. The attenuation functions are formulated so that they do not affect the normal-mode frequencies and harmonic force field. We previously found[40] at the level of quadratic configuration interaction with single, double, and perturbative corrections for triple excitations[47] with the correlation consistent polarized valence triple-ζ basis set of Dunning[48] (QCISD(T)/cc-pvtz) that the following exponential function describes the attenuation of bending force constants and the torsional barrier in $HONO_2$ as the HO−NO_2 distance is increased:

$$S(r) = \exp[-C(r - r_0)] \qquad (8)$$

This attenuation function does not affect the harmonic force field at the equilibrium bond distance, but it strongly influences the PES at longer distances, where the centrifugal barrier maximum is located. Thus, it is not surprising that the calculated capture rate constants are sensitive to the switching function parameters, as shown in Figure 4.

We investigated parameters in switching functions for the ∠HON harmonic bend, the ∠ONO harmonic bend, the HO−NO_2 torsion, and the wag modes. The *X*-axis in Figure 4 shows ratios of switching function parameters (compared to the standard PES; Table 1 of ref 40) used in modified PESs. The

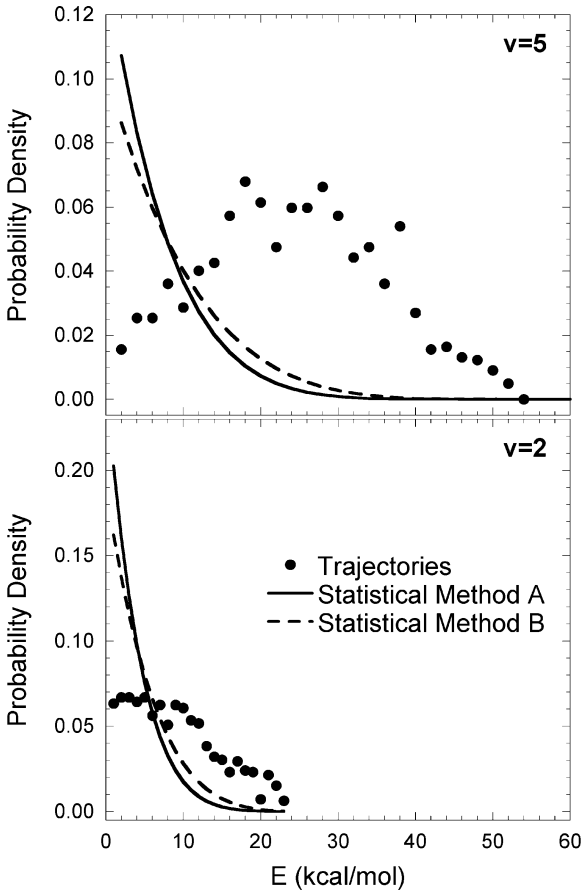

Figure 5. Vibrational energy distributions from trajectory calculations (standard PES) and statistical theory. Statistical methods A and B; see text for details.

Y-axis shows ratios of capture numbers (compared to the standard PES). As seen in Figure 4, the capture numbers increase with increasing switching function parameters, and then level off. It also appears that the capture numbers are highly sensitive to the switching parameters in harmonic bending modes. By changing the switching function parameters for the ∠HON and ∠ONO harmonic bending modes, the capture number can be increased by a factor of 3× to 5× . This is probably because increasing the switching function parameters results in attenuating the interaction faster as the newly formed O−N bond length increases. Therefore, the PES effectively has a broader acceptance angle when the O−N distance is large. This produces a larger rate constant.

3.3. Product OH(v') Vibrational Energy Distributions. In the present work no trajectory (out of batches of 10000 trajectories) resulted in a change of more than 0.25 kcal mol^{-1} in vibrational energy, unless a capture complex was formed. This result is consistent with the expected small rate constants for vibrational deactivation in collisions of OH(v) with nonreactive gases. In contrast, collisions that resulted in formation of a capture complex produced substantial vibrational energy deactivation, as shown by the representative energy distributions in Figure 5. All of the calculated energy distributions are very broad, corresponding to loss of about half of the vibrational excitation, regardless of the initial OH(v) vibrational level. When the initial vibrational level is high (e.g., $v = 5$), the energy distribution is peaked at intermediate energies; when it is low (e.g., $v = 2$), the energy distribution is peaked near zero energy. Because the energy distributions are not very sensitive to whether the PES is standard, stiff, or stiffer, other calculations are not shown.

In the following subsections, the energy distributions will be compared to statistical models and to the experimental data obtained by Hynes and co-workers.

Statistical Models. A comparison of the trajectory results with statistical theory (where IVR is assumed to be complete) can be used to ascertain whether the product energy distribution is affected by incomplete IVR and other factors. For this purpose, statistical models at two different levels of complexity are compared with the OH(v') vibrational energy distributions calculated via trajectories on the $HONO_2$ PESs. Many statistical approaches are possible, based on various statistical and dynamical assumptions.[38,54] For present purposes, we will only consider the prior distribution (method A) and the phase space distribution (method B).

In statistical method A (the prior distribution), we assume that the transient $HONO_2$ complex can be treated as an assembly of $n = 9$ classical harmonic oscillators, one of which is the OH stretch. As the complex dissociates, the portion of the randomized energy that is statistically distributed in the OH stretching mode of nitric acid appears in the OH(v') free radical product. Now assume that the nitric acid vibrations can be divided into two groups: a single mode (the OH stretch mode) and the n-1 remaining modes with corresponding densities of states (ρ_1 and ρ_{n-1}, respectively). The general expression[55] for the total density of states $\rho_n(E)$ for all n separable oscillators at total energy E is the convolution

$$\rho_n(E) = \int_0^E \rho_1(x)\rho_{n-1}(E - x)\,dx \tag{9}$$

where x is the energy in the single mode and $E - x$ is the energy in the $n - 1$ remaining modes. The probability that the energy in the single mode is in the range x to $x + dx$ when the total energy is held fixed at E is given by

$$P_1(x|E)\,dx = \frac{\rho_1(x)\rho_{n-1}(E - x)\,dx}{\int_0^E \rho_1(x)\rho_{n-1}(E - x)\,dx} \tag{10}$$

where $P_1(x|E)$ is the probability density distribution. For a collection of s separable classical harmonic oscillators, the density of states at total energy E is

$$\rho_s(E) = \frac{E^{s-1}}{(s-1)!\prod_{i=1}^{s} h\nu_i} \tag{11}$$

By substituting eq 11 into eq 10, one obtains the expression for the probability density that energy x resides in the OH mode when the total energy in $HONO_2$ or HOONO (where $n = 9$) is held fixed at E:

$$P_{OH}(x|E) = \frac{\rho_1(x)\rho_{n-1}(E - x)}{\rho_n(E)} = \frac{8(E - x)^7}{E^8} \tag{12}$$

A second statistical approach, phase space theory (statistical method B), is obtained by considering the statistical distribution of energy among the vibrations, translations, and rotations of the products, taking care to conserve both linear and angular momentum. This theory has been widely used to model product energy distributions in unimolecular reactions.[38] It is generally thought to be valid for relatively low available product energies and when the potential is nearly isotropic at distances greater than at the transition state, resulting in little perturbation of the product internal states.[54] The classical density of states for translations and rotations is proportional to $E^{(m-2)/2}$, where m is the number of translational or rotational degrees of freedom.[38] According to this approach, the distribution of vibrational energy in the product OH radical is given by the following expression:[38]

$$P'_{OH}(x|E)\,dx = \frac{\rho_{OH}(x)\,dx}{N(E)} \int_0^{E-x} \int_0^{E-x-E_t} \rho_t(E_t)\rho_r(E_r)\rho_{NO_2}(E - E_t - E_r - x)\,dE_r\,dE_t \tag{13}$$

where the $\rho_i(E_i)$ factors are densities of states at the corresponding energies for the product relative translations ($\rho_t(E_t)$), product rotations ($\rho_r(E_r)$), OH vibration ($\rho_{OH}(x)$), and NO_2 vibrations ($\rho_{NO_2}(E_v)$). The normalization factor $N(E)$ is given by

$$N(E) = \int_0^E \int_0^{E-E_t} \int_0^{E-E_t-E_r} \rho_t(E_t)\rho_r(E_r)\rho_{OH}(x)\rho_{NO_2}(E - E_t - E_r - x)\,dx\,dE_r\,dE_t \tag{14}$$

When momentum conservation laws are taken into account and the system is rotationally cold, the number of translational and rotational degrees of freedom can each be reduced by one, to a good approximation. As explained by Baer and Hase,[38] this is because conservation of linear momentum effectively reduces the number of relative translational degrees of freedom from 3 to 2 and because in the $J \rightarrow 0$ limit angular momentum conservation effectively reduces the number of product rotational degrees of freedom by one. Therefore, in this case there remain two translational degrees of freedom, a total of four rotational degrees of freedom for OH and NO_2, one vibrational degree of freedom for OH and three for NO_2. Using the expressions given above for the densities of states, the integrals in eqs 15 and 16 can be solved analytically to give

$$P'_{OH}(x|E) = \frac{6(E - x)^5}{E^6} \tag{15}$$

Predictions of the product OH(x) vibration energy distribution on the basis of the two statistical approaches are compared with the trajectory calculations in Figure 5. Both statistical approaches predict smooth monotonic functions with maximum values at $x = 0$ for the OH vibrational energy distribution. This behavior is due essentially to the fact that the density of vibrational states of diatomic OH is independent of energy; for a polyatomic, where the density of states is a strong function of energy, the function generally has a maximum at $x > 0$. Although somewhat noisy, the results from the trajectory calculations with initial $v = 2$ (Figure 5a) also appear to be described by a monotonic function with maximum near $x = 0$, but the distribution is not as sharply peaked as the statistical models. The trajectory results for initial $v = 5$ (Figure 5b) are peaked far from $x = 0$, in sharp contrast to these simple statistical models.

Vibrational Deactivation Efficiencies. When a $HONO_2$* complex is produced by the capture process, IVR takes place and may or may not be complete during the lifetime of the transient complex. Our previous work showed that IVR from the O−H bond in $HONO_2$ is highly dependent on internal energy.[40] Because energy is conserved, the transient complex has enough energy to re-dissociate to give OH(v') and NO_2. If IVR is too slow to randomize the energy that was initially resident in reactant OH(v), the product OH(v') will have nearly the same vibrational energy as the reactant, and vibrational deactivation will be deemed inefficient. However, for an ideal

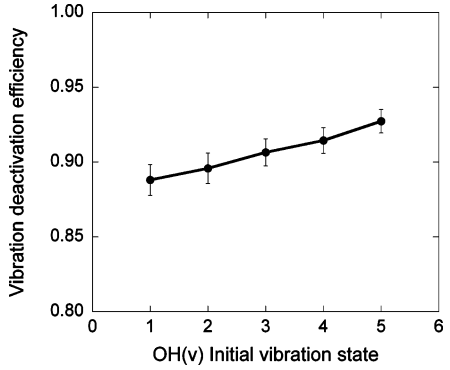

Figure 6. Vibrational deactivation efficiency as a function of OH(v) initial vibrational energy level (standard PES). Error bars show 1σ statistical errors.

strongly coupled complex, energy will be randomized before re-dissociation, resulting in a considerable loss of energy from the OH: vibrational deactivation will be deemed efficient. The vibrational deactivation efficiency η_v can be defined by the fraction of product OH(v'), where $v' \neq v$. The corresponding rate constant for vibrational deactivation via formation of a capture complex can be defined as $k_v = \eta_v k_{cap}$, where k_{cap} is the capture rate constant. For $\eta_v \approx 1$, the measured k_v can be used as a proxy for $k_{cap} = k_\infty$.

In trajectory calculations, the product OH vibrational quantum number v' can be assigned by binning the OH vibrational energy. The boundaries of each bin are chosen as the mean energy of two adjacent vibration energy levels. Using this approach, we can determine the vibration deactivation efficiencies. The product OH vibrational energy distributions resulting from collisions involving initial OH(v) vibrational energy states at $v = 2$ and $v = 5$ are shown in Figure 5 The corresponding vibration deactivation efficiencies are shown in Figure 6. In all cases, the vibration deactivation efficiencies are very high, ranging from $\eta_1 = 0.88$ to $\eta_5 = 0.92$. These calculated results show that $k_\infty \approx k_v/0.9$. Although the quantitative accuracy of this result is somewhat uncertain because of the limitations in the standard PES and in the energy binning of the trajectories, the conclusion that the deactivation efficiency is essentially independent of v appears to be a robust result.

Experimental tests[27−29] that show k_v to be independent of v provide convincing evidence that k_v can be used as a proxy for k_∞ for this reaction system. However, it is important to recognize that the two rate constants are probably proportional to each other, but not identically equal.

3.4. Lifetimes and Redissociation Rates. In the present trajectory calculations, the initial coordinates and momenta for the vibrations are selected according to microcanonical normal mode sampling (a standard VENUS option). Rotational and translational energies are selected from thermal distributions. It follows that each excited $HONO_2$* complex has a total internal energy governed by (a) the initial vibrational energies of the reactants, (b) the binding energy of the HO−NO_2 bond (classically 51.3 kcal mol^{-1}), and (c) the relative translational and rotational energies. Thus, the ensemble distribution of energies is not microcanonical, but it covers a range of energies in the vicinity of the ensemble average $\langle E \rangle$.

Because the initial total energy distribution of nascent complexes is not microcanonical, it is convenient to define ensemble average lifetime and re-dissociation rate constant for a given batch of trajectories:

$$\langle \tau(E) \rangle = \frac{1}{N} \sum_{i=1}^{N} \Delta t_i \tag{16a}$$

$$\langle k(E) \rangle = \frac{1}{N} \sum_{i=1}^{N} \frac{1}{\Delta t_i} \tag{16b}$$

where Δt_i is the time during which a HO−NO_2 capture complex exists during the ith trajectory and $\langle E \rangle$ is the average vibrational energy of complexes formed in the ensemble of trajectories:

$$\langle E \rangle = \frac{1}{N} \sum_{i=1}^{N} E_i \tag{16c}$$

Equation 16b follows from the fact that the rate constant of a first-order reaction is inversely proportional to the chemical lifetime, and the calculated Δt_i for a specific trajectory is the best measure of the lifetime that one can extract from a single trajectory. The ensemble average rate constant is therefore assumed to be equal to the ensemble average inverse lifetime (the result is not much different, however, from assuming that $\langle k(E) \rangle = \langle \tau(E) \rangle^{-1}$). By choosing different OH(v) and/or $NO_2(v_1v_2v_3)$ initial quantum states and temperatures, $\langle E \rangle$ can be varied, resulting in different average lifetimes and dissociation rate constants.

Figure 7 shows capture rate constants and lifetimes for different initial OH(v) energy levels. The capture rate constants are almost independent of v, but the average lifetimes show a strong dependence: the more energetic complexes dissociate much faster. As temperature is varied the same trend with energy is apparent. These results are qualitatively consistent with the energy-dependent specific rate constants from unimolecular reaction rate theory,[55−59] but it is not the purpose of the present work to make a detailed comparison between the classical trajectory calculations and transition state theory (TST). Several such comparisons have been made,[60] and the results often show good agreement with classical trajectory calculations carried out using the same PES.

The dissociation rate constants $\langle k(E) \rangle$ calculated from trajectories with initial OH(v) excitation are shown in Figure 8 as a function of energy. Additional calculations with initial excitation of NO_2 (instead of OH) are also shown in Figure 8. The trajectory results obtained using microcanonical normal mode sampling with various fixed energies [$NO_2(v_1v_2v_3)$ series A] give significantly different results at the same total energies than when OH(v) is initially excited. Three additional calculations carried out with arbitrary vibrational state combinations in NO_2 [$NO_2(v_1v_2v_3)$ series B] show additional differences among the redissociation rate constants.

If energy randomization is complete, the rate constants at a given energy should be independent of how the energy is distributed in the reactants. The present results show significant differences. These differences prove that the initial distribution of energy in the reactants strongly affects the calculated rate constants, probably because energy randomization is not complete prior to redissociation.

3.5. Peroxynitrous Acid (HOONO). In recent measurements of vibration relaxation of OH(v) by NO_2 at low pressures, Hynes and co-workers[27−29] found that the rate constant k_v for loss of OH(v) is almost independent of v. Their results are consistent with the trajectory calculations described above for the $HONO_2$ transient complex. However, the present trajectory calculations do not allow for formation of the transient HOONO complex, which should play a role in the experiments. Master equation

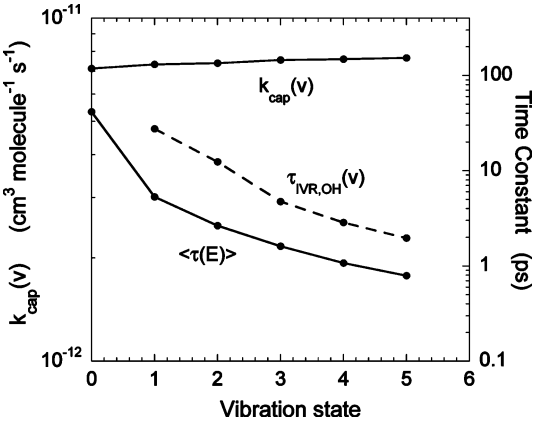

Figure 7. Capture rate constants ($k_{cap}(v)$) and lifetimes of complexes with respect to dissociation ($\langle\tau(E)\rangle$ from eq 16a) computed as a function of OH(v) initial vibrational state (standard PES). Also shown for comparison are calculated IVR lifetimes[40] ($\tau_{IVR,OH}(v)$) for excited states of the OH stretch mode in $HONO_2$ (where the other vibrational modes have only zero point energy).

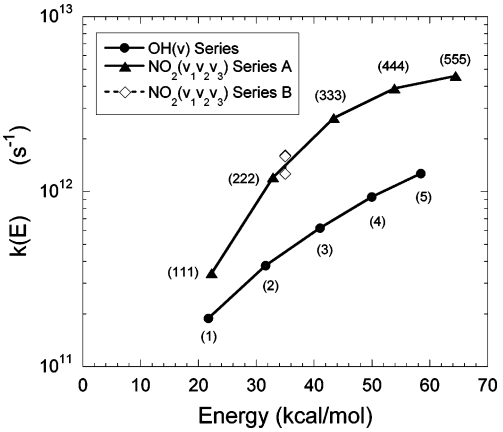

Figure 8. Dissociation rate constants $k(E)$ from trajectory calculations (standard PES; energy is relative to separated reactants at rest without zero point energy). Quantum numbers for OH(v) and $NO_2(v_1v_2v_3)$ series A are shown in the figure. The quantum numbers for $NO_2(v_1v_2v_3)$ series B are (910), (250), and (005) [although only two points are visible in the figure].

simulations[20] and theoretical analysis[26] of experimental data on the full reaction system estimate that the initial formation of HO−ONO is even more likely than formation of HO−NO_2. Thus, the experimental results of Hynes and co-workers[27−29] indicate that vibration deactivation via the HOONO* transient complex is also essentially independent of the initial OH(v) vibrational state. As discussed in the Introduction, isomerization from HOONO to $HONO_2$ is thought to be very slow.[19−21] Therefore, other reasons for the high efficiency must be sought.

One of the most important differences between HOONO and $HONO_2$ is the difference in strengths of the newly formed bonds: ∼80 kJ mol^{-1} for HO−ONO[14,20,61,62] vs ∼200 kJ mol^{-1} for HO−NO_2.[20,63] If one assumes that the difference in bond strength is the most important distinction between the two isomers, a crude method to investigate the vibrational deactivation efficiency via the HOONO channel is to artificially reduce the O−N bond strength in the $HONO_2$ standard PES described above. Trajectory calculations carried out in this way give vibrational deactivation efficiencies near unity for high initial vibrational energy levels in OH(v), but much lower efficiencies for low initial v. This result does not agree with the experiments carried out by Hynes and co-workers,[27−29] indicating that weakening the O−N bond in the $HONO_2$ PES does not yield a satisfactory PES for HOONO, possibly because of the contrast between chemical bonding in HOONO vs $HONO_2$.

The bonding in HOONO may produce stronger intermode coupling than in $HONO_2$. This may affect the relative rates of IVR and hence the relative vibrational deactivation efficiencies. In NO_2, which has C_{2v} symmetry, the two N−O bonds have equal force constants and equal equilibrium bond lengths. The same characteristics occur in $HONO_2$: the two terminal N−O bonds have essentially equal force constants and equilibrium bond lengths. Furthermore, these force constants in $HONO_2$ and in NO_2 are similar in magnitude. In HOONO, on the other hand, the terminal N−O is a double bond, while the interior N−O is a single bond. The two bonds have unequal force constants and unequal equilibrium bond lengths.[18,20,22,64−68] Thus, as the new HO−ONO bond is stretched, the ONO moiety goes from an asymmetric structure toward a symmetrical one. As a result, one would expect significant inter-mode coupling between vibrational modes that have important contributions from the O−O bond and the N−O bonds. Since the O−H bond is adjacent to the newly formed O−O bond, one might also expect relatively strong coupling between modes involving those two bonds. In addition it is important to note that HOONO has two unsymmetrical internal rotors and several conformers and that the *cis*,*cis*-HOONO conformer is a planar ring structure with an internal hydrogen bond to the terminal O atom.[64,65] This internal hydrogen bonding would also be expected to enhance intermode coupling with the OH bond.[68]

A number of other factors are important in controlling IVR rates in isolated molecules, as shown in many experimental and theoretical studies.[33,40,49,69−92] If resonances exist between an excited mode and overtones of lower frequency modes, the IVR rate tends to be enhanced. The magnitude of the rate enhancement depends on the details of the resonances. Such resonances have been implicated in IVR in $HONO_2$,[40] but a similar analysis for HOONO will require an accurate PES. It is also possible that conical intersections and coupling among electronic states can produce randomization of energy when electronic states are strongly coupled.[93] However, little is known about the possible electronic interactions in $HONO_2$ and HOONO.

Thus, there are reasons to surmise that energy in the OH bond of the nascent highly vibrationally excited adduct may be randomized more rapidly in HOONO than in $HONO_2$ due to enhanced intermode coupling. To test this conjecture is beyond the scope of the present work, since an accurate potential energy surface for HOONO will be required. However, the scant experimental evidence tends to contradict this conjecture, since optical excitation in the OH $v = 2$ overtone region in $HONO_2$ (at ∼6944 cm^{-1}) produces an IVR time constant of ∼12 ps,[49] while excitation of trans, perp-HOONO (at ∼6971 cm^{-1}) produces an apparent IVR time constant of ∼27 ps.[62] Thus, the mechanism for efficient IVR in HOONO is not known and must await the results of future work.

4. Discussion and Conclusions

The present results have a number of interesting features. The calculated capture rate constants depend only weakly on temperature and hardly at all on the initial vibrational excitation in OH(v). The weak temperature dependence is consistent with predictions made by Troe[21,26] and with variational transition state calculations on other recombination reactions.[94] An interesting feature of the present trajectory calculations is the "positive" activation energy (rate constant increasing with increasing temperature) for a barrierless reaction. One might have expected a "negative" activation energy (rate constant decreasing with

increasing temperature), since the PES is attractive in a barrierless reaction. We surmise that the positive activation energy results from trajectories with enough translational energy to surmount the low energy "ridges" on the PES that flank the entrance valley,[40] giving the entrance valley a wider acceptance angle at higher translational energies. In other words, the PES anisotropy is reduced at higher translational energy.

The capture process is not sensitive to the vibrational state of OH(v). Since there is no energy barrier to be surmounted, the energy in the "transitional modes" (the relative translations and rotations of the reactants) is sufficient for the capture reaction and the vibrations play essentially no role. Because the initial capture process is so fast, there is no time for significant coupling between the reaction coordinate and the other vibrational modes, yet IVR must be fast enough during the first vibrational period of the new bond so that enough energy is removed from the reaction coordinate and redissociation does not occur. The present results show that the reactant internal energy distributions can be far from equilibrium, yet the capture rate constant can remain the same as the equilibrium value. This is not true of the redissociation rate constant.

Redissociation requires surmounting an energy barrier. If sufficient energy is not present in the reaction coordinate, reaction cannot occur. Thus, the capture complex must live long enough for energy to find its way back into the reaction coordinate. The present results show that the rate of redissociation depends on where the energy resides. This is because there are at least two IVR time scales involved: the first is the time needed for the required energy to find its way back into the reaction coordinate from the pool of other modes. This is the IVR time scale for coupling between the reaction coordinate and the pool of other vibrations described by the local random matrix theory of Wolynes, Leitner, and their co-workers.[95−98] The second time scale is governed by the rate of IVR between relatively isolated modes (like the OH stretch) and the pool of remaining modes. This OH stretch mode IVR lifetime is shown for comparison in Figure 7. As we showed previously for nitric acid, energy initially resident in the OH stretch mode undergoes relatively rapid IVR,[40] but the present results show that this process is not fast enough to enable complete energy randomization during the lifetime of the capture complex.

How much energy remains stored in the OH mode when the capture complex dissociates? We can obtain a rough estimate of this quantity by comparing the redissociation rate constants from the different series in Figure 8. If we assume the rate constants obtained with $NO_2(v_1v_2v_3)$ excitation correspond to the fully randomized capture complex, we find that the rate constant calculated for OH($v = 5$) matches that obtained with NO_2 excitation if the energy is shifted by $\sim$25 kcal mol^{-1}. This energy shift is about half of the 46 kcal mol^{-1} energy difference between $v = 5$ and $v = 0$ for OH(v). The same approximate energy ratio is found for the other rate constants calculated with OH(v). Thus, we conclude that IVR from OH to the other modes is fast enough to randomize only about half of vibrational energy initially present in the OH mode, prior to redissociation. This conclusion is supported qualitatively by the lifetimes plotted in Figure 7. The OH stretch mode IVR lifetime is of the same order as the lifetime with respect to dissociation at the same level of OH vibrational excitation. This comparison is not completely straightforward, however, because the capture complex has a significantly higher total energy than the overtone-excited $HONO_2$ molecule.

The OH(v') energy distributions shown in Figure 5 are clearly different from the two statistical distributions used for comparison. This is consistent with slow randomization of energy and the dependence of the redissociation rate constant on the specific reactant vibrational states. At the higher energy (initial $v = 5$, Figure 5b), where the lifetime is very short, the statistical predictions are worse than at low energy ($v = 2$, Figure 5a), where the lifetime is much longer.

There are other possible reasons for why the calculated product OH(v') vibrational energy distributions are not statistical. A possible technical deficiency is that eqs 12 and 15 are based on the rigid rotor and harmonic oscillator approximations, in contrast to the PES used in the trajectory calculations. The PES is anharmonic and allows for centrifugal distortion. A second technical deficiency is that the densities of states in the above derivations are based on *separable* degrees of freedom, despite the strong coupling that must be present at high internal energies. These technical deficiencies may explain some quantitative discrepancies, but it seems unlikely that they can account for the qualitatively different behavior found for initial $v = 5$ (see Figure 5b). Slow IVR provides a more direct explanation.

It is quite possible that the effects of slow IVR are present, but not detected, in many (but not all[99,100]) reactions. As long as the energy content in an isolated degree of freedom like the OH stretch is relatively low (or nearly statistical), slow IVR will play little role in determining the reaction rate constant. It is well-known that, according to quantum statistics, high vibrational frequencies have little effect on entropy and densities of states; hence, they have little effect on reaction rate constants. If the amount of energy sequestered in an isolated vibrational mode is relatively small, the reaction rate constant may still be predicted reasonably accurately by statistical theory. However, in systems like the one investigated here, where large amounts of energy are placed in an isolated vibrational mode, the limitations due to slow IVR become apparent in the product energy distribution and in the rate of redissociation.

Despite the incomplete randomization of energy in the nitric acid capture complex, however, the efficiency of deactivating the initial OH(v) is still very high and independent of v, consistent with the experiments of Hynes and co-workers.[27−29] Note that the lack of dependence of vibrational deactivation efficiency on v does not necessarily mean that the capture complex is sufficiently "strongly coupled" for complete energy randomization prior to redissociation.

Of course, these calculations were carried out using a model potential energy surface, which, although accurate near the nitric acid equilibrium structure, is probably not highly accurate as the HO−NO_2 bond is stretched. However, the present results show that although the capture rate constant is sensitive to the switching functions and other details of the PES at long range, the final OH(v) vibrational energy distributions are practically unaffected. Moreover, our previous work showed that the IVR time constant for randomization of energy in the OH mode of nitric acid also shows very little sensitivity to such details.[40] Instead, it is mostly sensitive to the vibrational energy spectrum of the molecule. Thus, the results obtained here may be robust, even though the PES is not fully accurate.

When the HO−NO_2 bond is weakened to match that of the HO−ONO bond, the OH(v) deactivation efficiency becomes strongly dependent on v, unlike the experiments. This indicates that the inter-mode vibrational coupling in HOONO may be greater than in the weakened version of $HONO_2$, probably because of the difference in electronic structure and consequent differences in equilibrium bond lengths and force constants. It is also possible that the vibrational spectrum of HOONO promotes more Fermi resonances and faster IVR. In future work,

it will be important to construct a PES for HOONO and investigate how the multiple conformers affect the capture process, IVR, and vibrational deactivation efficiency. The HNO_3 chemical system continues to provide a rich area for study.

Acknowledgment. This paper celebrates the continuing career of Bill Hase, who has long been a leader in classical trajectory calculations and in the study of IVR. Thanks go to A. J. Hynes for a copy of ref 27 prior to publication. J.R.B. thanks David Golden, Mitchio Okumura, Anne McCoy, Barney Ellison, and John Stanton for stimulating discussions about the HNO_3 reaction system. Thanks also go to Yurdanur Turker (summer undergraduate researcher funded in part by the University of Michigan) for her contributions to our (so far unsuccessful) attempts to develop a HOONO potential energy surface. We also thank two anonymous referees for some helpful suggestions. Finally, we are grateful to NASA (Upper Atmosphere Research Program) and NSF (Atmospheric Chemistry Division) for funding. [This material is based upon work supported in part by the National Science Foundation under Grant No. 0344102. Any opinions, findings, and conclusions or recommendations expressed in this material are those of the authors and do not necessarily reflect the views of the National Science Foundation.]

References and Notes

(1) Quack, M.; Troe, J. *Ber. Bunsen-Ges. Phys. Chem.* **1975**, *79*, 170.
(2) Jaffer, D. H.; Smith, I. W. M. *J. Chem. Soc., Faraday Trans.* **1979**, *67*, 201.
(3) Smith, I. W. M. *J. Chem. Soc., Faraday Trans.* **1997**, *93*, 3741−3750.
(4) Herzfeld, K. F.; Litovitz, T. A. *Absorption and Dispersion of Ultrasonic Waves*; Academic Press: New York, 1959.
(5) Lambert, J. D. *Vibrational and Rotational Relaxation in Gases*; Clarendon Press: Oxford, U.K., 1977.
(6) Yardley, J. T. *Introduction to Molecular Energy Transfer*; Academic Press: New York, 1980.
(7) Shroll, R. M.; Lohr, L. L.; Barker, J. R. *J. Chem. Phys.* **2001**, *115*, 4573−4585.
(8) Dyer, M. J.; Knutsen, K.; Copeland, R. A. *J. Chem. Phys.* **1997**, *107*, 7809−7815.
(9) Wine, P. H.; Kreutter, N. M.; Ravishankara, A. R. *J. Phys. Chem.* **1979**, *83*, 3191−3195.
(10) Fulle, D.; Hamann, H. F.; Hippler, H.; Troe, J. *J. Chem. Phys.* **1998**, *108*, 5391−5397.
(11) Brown, S. S.; Talukdar, R. K.; Ravishankara, A. R. *Chem. Phys. Lett.* **1999**, *299*, 277.
(12) Dransfield, T. J.; Perkins, K. K.; Donahue, N. M.; Anderson, J. G.; Sprengnether, M. M.; Demerjian, K. L. *Geophys. Res. Lett.* **1999**, *26*, 687−690.
(13) Anastasi, C.; Smith, I. W. M. *J. Chem. Soc., Faraday Trans. 2* **1976**, *72*, 1459−1468.
(14) Hippler, H.; Nasterlack, S.; Striebel, F. *Phys. Chem. Chem. Phys.* **2002**, *4*, 2959−2964.
(15) Nizkorodov, S. A.; Wennberg, P. O. *J. Phys. Chem. A* **2002**, *106*, 855−859.
(16) Robertshaw, J. S.; Smith, I. W. M. *J. Phys. Chem.* **1982**, *86*, 785−790.
(17) Smith, G. P.; Golden, D. M. *Int. J. Chem. Kinet.* **1978**, *10*, 489.
(18) Fry, J. L.; Nizkorodov, S. A.; Okumura, M.; Roehl, C. M.; Francisco, J. S.; Wennberg, P. O. *J. Chem. Phys.* **2004**, *121*, 1432−1448.
(19) Barker, J. R.; Lohr, L. L.; Shroll, R. M.; Reading, S. *J. Phys. Chem. A.* **2003**, *107*, 7434−7444.
(20) Golden, D. M.; Barker, J. R.; Lohr, L. L. *J. Phys. Chem. A* **2003**, *107*, 11057−11071.
(21) Troe, J. *Int. J. Chem. Kinet.* **2001**, *33*, 878−889.
(22) Sumathy, R.; Peyerimhoff, S. D. *J. Chem. Phys.* **1997**, *107*, 1872−1880.
(23) Zhao, Y.; Houk, K. N.; Olsen, L. P. *J. Phys. Chem. A* **2004**, *108*, 5864−5871.
(24) Ellison, G. B.; Herbert, J. M.; McCoy, A. B.; Szalay, P. G.; Stanton, J. F. *J. Phys. Chem. A* **2004**, *108*, 7639−7642.
(25) Butkovskaya, N. I.; Kukui, A.; Pouvesle, N.; Le Bras, G. *J. Phys. Chem. A.* **2005**, *109*, 6509−6520.
(26) Troe, J. *Chem. Rev.* **2003**, *103*, 4565−4576.
(27) D'Ottone, L.; Bauer, D.; Campuzano-Jost, P.; Fardy, M.; Hynes, A. J. *Discuss. Faraday Soc.* **2005**, *130*, 111−123.
(28) D'Ottone, L.; Campuzano-Jost, P.; Bauer, D.; Hynes, A. J. *J. Phys. Chem. A* **2001**, *105*, 10538−10543.
(29) Silvente, E.; Richter, R. C.; Hynes, A. J. *J. Chem. Soc., Faraday Trans.* **1997**, *93*, 2821−2830.
(30) Guo, Y.; Thompson, D. L.; Sewell, T. D. *J. Chem. Phys.* **1996**, *104*, 576−582.
(31) Kabadi, V. N.; Rice, B. M. *J. Phys. Chem. A* **2004**, *108*, 532.
(32) Toselli, B. M.; Barker, J. R. *Chem. Phys. Lett.* **1990**, *174*, 304−308.
(33) Lu, D. H.; Hase, W. L. *J. Chem. Phys.* **1986**, *85*, 4422.
(34) Mullin, A. S.; Schatz, G. C. Dynamics of highly excited states in chemistry: An overview. In *Highly Excited States: Relaxation, Reaction, and Structure*; Mullin, A., Schatz, G. C., Eds.; American Chemical Society: Washington, DC, 1997; Vol. 678; pp 2−25.
(35) Schatz, G. C. *J. Phys. Chem.* **1995**, *99*, 516−524.
(36) Flynn, G. W.; Parmenter, C. S.; Wodtke, A. M. *J. Phys. Chem.* **1996**, *100*, 12817.
(37) Oref, I.; Tardy, D. C. *Chem. Rev.* **1990**, *90*, 1407.
(38) Baer, T.; Hase, W. L. *Unimolecular Reaction Dynamics. Theory and Experiments*; Oxford University Press: New York, 1996.
(39) Yoder, L. M.; Barker, J. R. *J. Phys. Chem. A* **2000**, *104*, 10184−10193.
(40) Liu, Y.; Lohr, L. L.; Barker, J. R. *J. Phys. Chem. B* **2005**, *109*, 8304−8309.
(41) Duchovic, R. J.; Hase, W. L. *Chem. Phys. Lett.* **1984**, *110*, 474−477.
(42) Wang, Y.; Hase, W. L.; Wang, H. *J. Chem. Phys.* **2003**, *118*, 2688.
(43) Hase, W. L.; Darling, C. L.; Zhu, L. *J. Chem. Phys.* **1992**, *96*, 8295−8306.
(44) Porter, R. N.; Raff, L. M. Classical Trajectory methods in Molecular Collisions. In *Dynamics of Molecular Collisions*; Miller, W. H., Ed.; Plenum Press: New York and London, 1976; Vol. Part, B.
(45) Sewell, T. D.; Thompson, D. L. *Int. J. Mod. Phys. B* **1996**, *11*, 1067.
(46) Frisch, M. J.; Trucks, G. W.; Schlegel, H. B.; Scuseria, G. E.; Robb, M. A.; Cheeseman, J. R.; Zakrzewski, V. G.; Montgomery, J.; Stratmann, R. E.; Burant, J. C.; Dapprich, S.; Millam, J. M.; Daniels, A. D.; Kudin, K. N.; Strain, M. C.; Farkas, O.; Tomasi, J.; Barone, V.; Cossi, M.; Cammi, R.; Mennucci, B.; Pomelli, C.; Adamo, C.; Clifford, S.; Ochterski, J.; Petersson, G. A.; Ayala, P. Y.; Cui, Q.; Morokuma, K.; Malick, D. K.; Rabuck, A. D.; Raghavachari, K.; Foresman, J. B.; Cioslowski, J.; Ortiz, J. V.; Baboul, A. G.; Stefanov, B. B.; Liu, G.; Liashenko, A.; Piskorz, P.; Komaromi, I.; Gomperts, R.; Martin, R. L.; Fox, D. J.; Keith, T.; Al-Laham, M. A.; Peng, C. Y.; Nanayakkara, A.; Challacombe, M.; Gill, P. M. W.; Johnson, B.; Chen, W.; Wong, M. W.; Andres, J. L.; González, C.; Head-Gordon, M.; Replogle, E. S.; Pople, J. A. Gaussian 98, Revision A.7. Gaussian Inc.: Pittsburgh, PA, 1998.
(47) Pople, J. A.; Head-Gordon, M.; Raghavachari, K. *J. Chem. Phys.* **1987**, *87*, 5968−5975.
(48) Woon, D. E.; Dunning, T. H., Jr. *J. Chem. Phys.* **1993**, *98*, 1358−1371.
(49) Bingemann, D.; Gorman, M. P.; King, A. M.; Crim, F. F. *J. Chem. Phys.* **1997**, *107*, 661.
(50) Hase, W. L.; Duchovic, R. J.; Hu, X.; Komornicki, A.; Lim, K. F.; Lu, D.-H.; Peslherbe, G. H.; Swamy, K. N.; Linde, S. R. V.; Varandas, A.; Wang, H.; Wolf, R. J. *Quant. Chem. Prog. Exch. Bull.* **1996**, *16*, 43.
(51) Schatz, G. C. *Rev. Mod. Phys.* **1989**, *61*, 669−688.
(52) Peslherbe, G. H.; Wang, H.; Hase, W. L. *Adv. Chem. Phys.* **1999**, *105*, 171.
(53) NIST. *Chemistry WebBook: NIST Standard Reference Database Number 69*, March 2003 ed.; National Institute of Science and Technology: Gaithersburg, MD, 2003.
(54) Bonnet, L.; Larregaray, P.; Rayez, J.-C. *Phys. Chem. Chem. Phys.* **2005**, *7*, 3540−3544.
(55) Forst, W. *Theory of Unimolecular Reactions*; Academic Press: New York, 1973.
(56) Forst, W. *Unimolecular Reactions. A Concise Introduction*; Cambridge University Press: Cambridge, U.K., 2003.
(57) Gilbert, R. G.; Smith, S. C. *Theory of Unimolecular and Recombination Reactions*; Blackwell Scientific: Oxford, U.K., 1990.
(58) Holbrook, K. A.; Pilling, M. J.; Robertson, S. H. *Unimolecular Reactions*, 2 ed.; Wiley: Chichester, U.K., 1996.
(59) Robinson, P. J.; Holbrook, K. A. *Unimolecular Reactions*; Wiley-Interscience: New York, 1972.
(60) Truhlar, D. G.; Garrett, B. C.; Klippenstein, S. J. *J. Phys. Chem.* **1996**, *100*, 12771−12800.
(61) Golden, D. M.; Barker, J. R.; Lohr, L. L. *J. Phys. Chem. A* **2004**, *108*, 8552.
(62) Konen, I. M.; Pollack, L. B.; Li, E. X. J.; Lester, M. I.; Varner, M. E.; Stanton, J. F. *J. Chem. Phys.* **2005**, *122*, 094320.

(63) Dorofeeva, O. V.; Iorish, V. S.; Novikov, V. P.; Neuman, D. B. *J. Phys. Chem. Ref. Data* **2003**, *32*, 879−901.
(64) McGrath, M. P.; Rowland, F. S. *J. Phys. Chem.* **1994**, *98*, 1061−1067.
(65) McGrath, M. P.; Rowland, F. S. *J. Chem. Phys.* **2005**, *122*, 134312.
(66) Bean, B. D.; Mollner, A. K.; Nizkorodov, S.; Nair, G.; Okumura, M.; Sander, S. P.; Peterson, K. A.; Francisco, J. S. *J. Phys. Chem. A* **2003**, *107*, 6974−6985.
(67) Mathews, J.; Sinha, A.; Francisco, J. S. *J. Chem. Phys.* **2004**, *120*, 10543−10553.
(68) McCoy, A. B.; Fry, J. L.; Francisco, J. S.; Mollner, A. K.; Okumura, M. *J. Chem. Phys.* **2005**, ***122***, 104311.
(69) Oref, I.; Rabinovitch, B. S. *Acc. Chem. Res.* **1979**, *12*, 166−175.
(70) Nesbitt, D. J.; Field, R. W. *J. Phys. Chem.* **1996**, *100*, 12735.
(71) Myers, D. J.; Shigeiwa, M.; Fayer, M. D.; Silbey, R. *Chem. Phys. Lett.* **1999**, *312*, 399.
(72) Yoo, H. D.; DeWitt, M. J.; Pate, B. H. *J. Phys. Chem. A* **2004**, *108*, 1348.
(73) Baskin, J. S.; Banares, L.; Pedersen, S.; Zewail, A. H. *J. Phys. Chem.* **1996**, *100*, 11920−11933.
(74) Felker, P. M.; Lambert, W. R.; Zewail, A. H. *J. Chem. Phys.* **1985**, *82*, 3003.
(75) Lehmann, K. K.; Scoles, G.; Pate, B. H. *Annu. Rev. Phys. Chem.* **1994**, *45*, 241.
(76) Page, R. H.; Shen, Y. R.; Lee, Y. T. *J. Chem. Phys.* **1988**, *88*, 5362.
(77) Callegari, A.; Srivastave, H. K.; Merker, U.; Lehmann, K. K.; Scoles, G.; Davis, M. J. *J. Chem. Phys.* **1997**, *106*, 432.
(78) Bakker, H. J.; Planken, P. C. M.; Kuipers, L.; Langendijk, A. *J. Chem. Phys.* **1990**, *94*, 1730.
(79) Seifert, G.; Zürl, R.; Patzlaff, T.; Graener, H. *J. Chem. Phys.* **2000**, *112*, 6349.
(80) Giebels, I. A. M. E.; van den Broek, M. A. F. H.; Kropman, M. F.; Bakker, H. J. *J. Chem. Phys.* **2000**, *112*, 5127.
(81) Iwaki, L. K.; Dlott, D. D. *J. Phys. Chem. A* **2000**, *104*, 9101.
(82) Iwaki, L. K.; Dlott, D. D. *Chem. Phys. Lett.* **2000**, *321*, 419.
(83) Assmann, J.; Benten, R. V.; Charvat, A.; Abel, B. *J. Phys. Chem. A* **2003**, *107*, 1904.
(84) Assmann, J.; Charvat, A.; Schwarzer, D.; Kappel, C.; Luther, K.; Abel, B. *J. Phys. Chem. A* **2002**, *106*, 5197−5201.
(85) Cheatum, C. M.; Heckscher, M. M.; Bingemann, D.; Crim, F. F. *J. Chem. Phys.* **2001**, *115*, 7086.
(86) Deak, J. C.; Iwaki, L. K.; Dlott, D. D. *J. Phys. Chem. A* **1999**, *103*, 971.
(87) Bintz, K. L.; Thompson, D. L.; Brady, J. W. *J. Chem. Phys.* **1987**, *86*, 4411.
(88) Gruebele, M. *Adv. Chem. Phys.* **2000**, *114*, 193.
(89) Gruebele, M. *Theor. Chem. Acc.* **2003**, *109*, 53−63.
(90) Gruebele, M.; Wolynes, P. G. *Acc. Chem. Res.* **2004**, *37*, 261−267.
(91) Rice, S. A. *Adv. Chem. Phys.* **1981**, *47*, 117.
(92) Uzer, T.; Miller, W. H. *Phys. Rep.* **1991**, *199*, 73−146.
(93) Smith, I. W. M. *Acc. Chem. Res.* **1976**, *9*, 161−168.
(94) Pesa, M.; Pilling, M. J.; Robertson, S. H.; Wardlaw, D. M. *J. Phys. Chem. A* **1998**, *102*, 8526−8536.
(95) Leitner, D. M.; Wolynes, P. G. *J. Chem. Phys.* **1996**, *105*, 11226−11236.
(96) Leitner, D. M.; Wolynes, P. G. *Abstracts of Papers of the American Chemical Society*; American Chemical Society: Washington, DC, 1996; Vol. 212, 58-PHYS.
(97) Leitner, D. M.; Wolynes, P. G. *Chem. Phys. Lett.* **1997**, *280*, 411−418.
(98) Leitner, D. M.; Levine, B.; Quenneville, J.; Martinez, T. J.; Wolynes, P. G. *J. Phys. Chem. A* **2003**, *107*, 10706−10716.
(99) Kiefer, J. H.; Katapodis, C.; Santhanam, S.; Srinivasan, N. K.; Tranter, R. S. *J. Phys. Chem. A* **2004**, *108*, 2443−2450.
(100) Barker, J. R.; Stimac, P. J.; King, K. D.; Leitner, D. M. *J. Phys. Chem. A* **2005**, in press.